Available online at www.sciencedirect.com

ScienceDirect

Procedia Structural Integrity 29 (2020) 95–102

Structural Integrity Procedia

www.elsevier.com/locate/procedia

Art Collections 2020, Safety Issue (ARCO 2020, SAFETY)

Comparative Assessment on the Rocking Response of Seismically Base-Isolated Rigid Blocks

Davide Pellecchia*[a], Salvatore Sessa[a], Nicolò Vaiana[a], Luciano Rosati[a]

[a]*Department of Structures for Engineering and Architecture, University of Naples Federico II, via Claudio 21, 80125 - Naples, Italy*

Abstract

In this work we investigate the rocking response of the Riace bronze A, a slender statue modelled as an equivalent rigid body freestanding on an isolated base supported on: (a) Steel Reinforced Elastomeric Bearings, (b) Fiber Reinforced Elastomeric Bearings, (c) Flat Surface Sliding Bearings, and (d) Curved Surface Sliding Bearings. The dynamic responses of such devices contribute significantly to the rocking response of the base-isolated rigid block, so it is necessary to accurately predict the complex hysteretic behaviors of the above-mentioned devices. For this reason, an innovative uniaxial phenomenological model has been used. The proposed hysteretic model is described by an algebraic equation that does not require iterations to evaluate the state variables, namely the device restoring forces. Moreover, the proposed hysteretic model is based on a set of parameters with a clear mechanical significance.

Peer-review under responsibility of Marco Tanganelli and Stefania Viti

Keywords: art object, hysteresis, nonlinear dynamics, rigid block, seismic isolation;

Introduction

A topic of great interest during the last two decades has been the mitigation of seismic risk for freestanding slender objects because many statues contained within museums are simply supported on the floor or a pedestal and are not prepared to handle the oscillations induced by earthquakes (Augusti 1992, Caliò 2004, Zuccaro 2017). The two main types of response of the art object (modelled as a rigid block) are sliding and rocking motions. The first researcher to

* Corresponding author. Tel.: +39 081-7683723;
E-mail address: davide.pellecchia@unina.it

Peer-review under responsibility of Marco Tanganelli and Stefania Viti
10.1016/j.prostr.2020.11.144

study the rocking response taking into account the collisions a rigid body is Housner (1963). However, between the above-mentioned motions, the most worrying is the rocking (Gesualdo 2016, Gesualdo 2018) because it could end up overturning the rigid body. Therefore, only the rocking response of rigid bodies is of specific interest in this paper.

In particular cases, some isolation systems have been developed for museum artifacts, such as the ones for the two statues known as Bronzes of Riace at the Archaeological Museum of Reggio Calabria (Italy) (De Canio 2012). In general, this kind of protection is expensive and for this reason, most artifacts are not equipped to mitigate seismic risk.

In this paper, the rocking response of the Riace bronze A modeled as a rigid body freestanding on an isolated base is investigated by employing four typologies of seismic devices, namely Steel Reinforced Elastomeric Bearings (SREBs), Fiber Reinforced Elastomeric Bearings (FREBs), Flat Surface Sliding Bearings (FSSBs), and Curved Surface Sliding Bearings (CSSBs). It is important to adopt a hysteretic model able to predict the complex hysteretic behavior of the seismic isolators since such devices are characterized by different shapes of the force-displacement hysteresis loop. For this reason, we have used some recently developed hysteretic models (Vaiana 2018, 2019a, 2019b, 2019c) of algebraic nature and based on a small set of parameters having a clear mechanical significance.

1. Problem statement

In this section, the system under investigation, namely the base-isolated rigid body, will be outlined. Accordingly, its properties, its kinematics, the equations of motion, and the formulation of the collisions of the model are presented.

1.1. Model's properties

The Riace bronze A has been modelled as a symmetric rigid body (as shown in Fig. 1(a) - of mass m, and rotational inertia about its centre of mass I- simply supported on a seismically isolated rigid base with mass m_b. The damping properties of the seismic isolation devices are modelled with a rate-independent hysteretic model with parameters having a clear mechanical significance. The rigid body has height and width equal to $2h$ and $2b$, respectively, and the distance from the centre of mass to one corner of its base is denoted by $R = \sqrt{b^2 + h^2}$. Finally, when the body is at rest, the distance R tilts relative to the vertical of an angle denoted by $\alpha = \tan^{-1}(b/h)$.

1.2. Model's kinematics

The rigid body could exhibit two possible dynamic responses when subject to ground excitation, namely sliding and rocking motions. Let us consider that the coefficient of kinetic friction between the body and the base is big enough to prevent the sliding motion. This assumption is motivated by the fact that between the above-mentioned motions, the most worrying is the rocking because it could end up overturning the rigid body. Consequently, the system has only two degrees of freedom, one relative to the rocking of the body about one of the two bottom corners, namely O and O', and the other corresponding to the relative horizontal displacement between the isolated base and the ground.

Regarding Fig. 1(b), the parameters that describe the above-mentioned motion are θ, to measure the tilting of the rigid body, and u, to measure the horizontal displacement between the isolated base and the ground.

1.3. Equation of motions

The equations of motion of the system subjected to horizontal ground excitation $\ddot{u}_g$ are

$$I_O\ddot{\theta} + m\left(\ddot{u}_g + \ddot{u}\right)R\cos(\operatorname{sgn}(\theta)\alpha - \theta) = -mgR\sin(\operatorname{sgn}(\theta)\alpha - \theta) \tag{1}$$

$$m(\ddot{u}_g + \ddot{u} + \ddot{x}) + m_b(\ddot{u}_g + \ddot{u}) + n_d c\dot{u} + n_d f_r = 0 \tag{2}$$

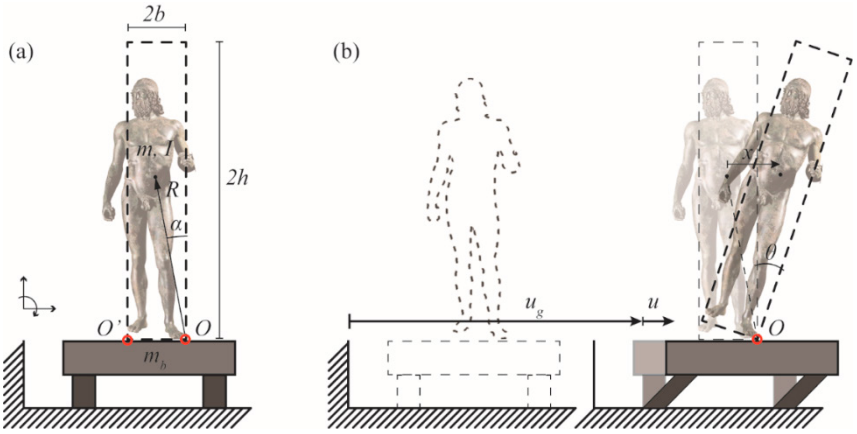

Fig. 1 - The proposed model and its kinematics.

The Eq. (1) is given by applying Newton's second law to the circular motion. The parameter I_O is the rotational inertia about the bottom corner $O(O')$, whereas, g denotes the gravitational acceleration. The Eq. (2) is given by applying Newton's second law to the horizontal direction. The parameter n_d is the number of the seismic isolation devices, c denotes the viscous damping coefficient of each seismic isolation device, and f_r is the restoring force of each seismic isolation device.

1.4. The collision conditions

When the angular displacement θ approaches zero, the rigid body will collide with the base-isolated rigid block. The motion of the rigid body changes suddenly when the collision occurs making the Eqs. (1) and (2) invalid and accordingly, in the dynamic response of the system there will be some discontinuities.

To compare the motion before and after the collision, the law of conservation of linear(angular) momentum is used. Indeed, although the kinetic energy decreases, the linear(angular) momentum remains unchanged. The loss of rotational kinetic energy in the collision of a base-isolated rigid body is:

$$r = \left(\frac{1}{2} I_O \dot{\theta}_i^2\right) / \left(\frac{1}{2} I_O \dot{\theta}_f^2\right) = \left(\frac{m^2(b^2+R^2) + 2b^2 m m_b - I_O(m+m_b)}{h^2 m^2 - I_O(m+m_b)}\right)^2 \tag{3}$$

Roussis (2008) have reached a similar expression delivering the rotational inertia I_O for rectangular body.

Concerning the base excitation, Eq. (1) has been formulated by accounting for a single horizontal seismic component. The vertical seismic component has been neglected despite of its pivotal role in overturning problems (Cimellaro 2020, Gesualdo 2018) since the present contribution aims to compare the performances of four typologies of insulation devices. A proper model accounting for the vertical ground motion must include a three-dimensional characterization of the mechanics of such devices. Because of the lack of exhaustive experimental data, the seismic vertical component is not considered in this research although it will be the focus of future research activities.

2. Isolation systems

The elastomeric and sliding bearings represent the main categories of seismic isolation devices used to date for seismic protection of art objects. There are significant differences between the two above-mentioned categories of isolation devices, especially in terms of hysteretic behavior. For this reason, in this section we will examine briefly the main characteristics of the elastomeric and sliding bearings with particular regard to description of the hysteretic behavior.

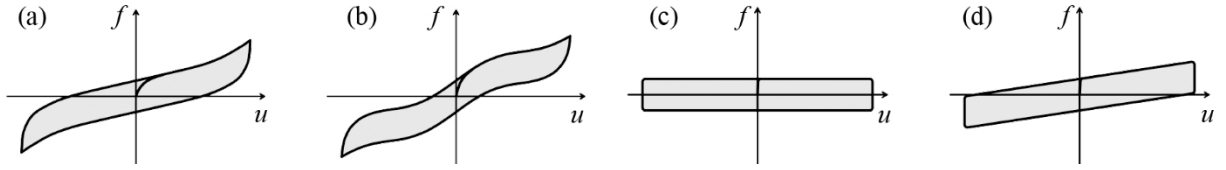

Fig. 2 - Typical hysteresis loop shapes of SREBs (a), FREBs (b), FSSBs (c), and CSSBs (d)

2.1. Steel Reinforced Elastomeric Bearings

Steel Reinforced Elastomeric Bearings have a circular or square transverse cross section and between the sheets of elastomer materials, there are some thin steel reinforcing plates. Such devices are connected with the superstructure and the substructure through two steel plates that bounded the top and the bottom surfaces of devices. The connection occurs typically with bolted bearings (Constantinou 2007). The behavior of SREBs displays symmetric hysteresis loops bounded between two parallel curves, generally characterized by kinematic hardening since the restoring force increases with increasing transverse displacement, see Fig. 2(a).

2.2. Fiber Reinforced Elastomeric Bearings

Fiber Reinforced Elastomeric Bearings have a rectangular, circular or square transverse cross section and between the sheets of elastomer materials, there are some fiber reinforcements. These fibers can be in carbon, glass, nylon, and polyester, and the fabric texture can be bi-axial or quadri-axial depending on whether the fiber follows two or four directions, respectively. Typically, FREBs are connected with the superstructure and the substructure without any type of chemical or mechanical bonding. The behavior of FREBs displays symmetric hysteresis loops bounded between two parallel curves, generally characterized by kinematic hardening since the restoring force increases with increasing transverse displacement, and by three or more inflection point according to the values of shear strains, Fig. 2(b).

2.3. Flat Surface Sliding Bearings

Flat Surface Sliding Bearings are characterized by an upper sliding plate, typically covered by Teflon, and a lower stainless steel plate. The Fig. 2(c) shows the typical hysteresis loop shape displayed by FSSBs. Many experiment results (Constantinou 1990, Mokha 1990) show that these devices present both types of hysteresis behaviors, namely, rate-dependent and rate-independent hysteretic behaviors. So that means that the device restoring force depends on the device transverse displacement as well as the device transverse velocity.

2.4. Curved Surface Sliding Bearings

Curved Surface Sliding Bearings, also known as Friction Pendulum Bearing, are characterized by a pendulum, typically covered by a low-friction composite material, that slides on a curved sliding surface. These devices as well as the FREBs, present both rate-dependent and rate-independent hysteretic behaviors. The Fig. 2(d) shows the typical hysteresis loop shape displayed by CSSBs.

2.5. Computational model

The nonlinear behavior of the base-isolated rigid block depends on the strongly hysteretic behavior characterizing the adopted seismic isolators. Accordingly, it is important to adopt an hysteretic model able to predict the complex hysteretic behavior of the seismic isolators. For this reason we have adopted hysteretic models belonging to a class recently developed by Vaiana (2018, 2019a, 2019b). Such constitutive model is of algebraic nature; thus, the device restoring force can be computed in closed form. Compared with constitutive models providing similar hysteresis shapes, such as the popular Bouc - Wen, the used model does not require any iterative procedure within each step of

the analysis. Moreover, it requires a smaller number of parameters having clear mechanical significance and it is able to account for the dependency of the response on the sliding velocity, bearing pressure and on the conditions of the interface. The chance of controlling such variegated behaviors makes such a model to be very accurate and computationally efficient in reproducing the actual behavior of the employed seismic devices.

Making reference to Vaiana (2018) for the details, the used model is based on five constitutive parameters. Such a formulation is sufficiently accurate to model the behavior of FREB and SREB devices, while sliding bearing response require a modified formulation presented in Vaiana (2019b) in which the sliding bearing restoring force strongly depends on the friction and it may be evaluated as Mokha (1990)

$$f(u,\dot{u}) = \frac{F_N}{r}u + \mu_k(\dot{u})F_N z(u) \tag{4}$$

where F_N is the normal compressive force, i.e. the force component acting perpendicular to the sliding surface, r is the radius of curvature of sliding surface, $\mu_k(\dot{u})$ is the coefficient of kinetic friction, on the other hand u and $\dot{u}$ are the bearing transverse displacement and velocity, respectively.

The expression to evaluate the coefficient of kinetic friction $\mu_k(\dot{u})$ is shown by Constantinou (1990).

3. Numerical experiments

Numerical experiments have been carried out to evaluate the response of the above-described system under horizontal ground excitation. The numerical solutions of the equations of motion (1) and (2) are done in MATLAB by using the explicit fourth-order Runge-Kutta method and applying the hysteretic models described in Sec. 2.5 to evaluate the device restoring force for each device analyzed. The collision condition is checked in each time step; in case of collision the procedure is restarted with the initial conditions for the angular displacement, the angular velocity, the transverse displacement and the transverse velocity immediately after the collision.

The nonlinear dynamic behavior of the base-isolated rigid body is computed by applying the E-W component of horizontal ground acceleration during the Irpinia earthquake of November 1980 as input.

3.1. Properties of the system

The numerical experiments' result has been obtained for the system illustrated in Fig. 1. The geometrical properties of the Riace bronze A were obtained by De Canio (2012). In particular the statue has mass $m = 185$ kg, and rotational inertia about its centre of mass $I = 54\,\mathrm{kg\,m^2}$, whereas the rigid base has mass $m_b = 4320$ kg. For each category of seismic isolation device described in Sec. 2, four values of the displacement limit have been selected, denoted as u_{lim}, from 100 mm to 400 mm. The mechanical properties of each device, and for each value of the displacement limit were derived from a factory's catalog. The hysteretic model parameters listed in Tab. 1 have been selected in order to obtain the maximum device restoring force shown by the factory's catalog.

Tab. 1 - Hysteretic model parameters.

Isolation seismic device	Limit displacement [m]	k_a [N m^{-1}]	k_b [N m^{-1}]	α	β_1 [N m^{-3}]	β_2 [N m^{-5}]
SREB	0.1	4.38×10^6	7.00×10^4	100	5.00×10^5	5.00×10^5
	0.2	4.39×10^6	7.00×10^4	100	5.00×10^5	5.00×10^5
	0.3	4.40×10^6	7.00×10^4	100	5.00×10^5	5.00×10^5
	0.4	1.00×10^7	2.25×10^5	100	5.00×10^5	5.00×10^5
FREB	0.1	3.10×10^6	2.00×10^5	100	-5.00×10^6	5.00×10^7
	0.2	3.20×10^6	2.00×10^5	100	-5.00×10^6	5.00×10^7
	0.3	7.70×10^6	2.00×10^5	100	-5.00×10^6	5.00×10^7
	0.4	1.00×10^7	4.50×10^5	100	-1.00×10^7	1.00×10^8

Isolation seismic device	Limit displacement [m]	k_a [N m^{-1}]	k_b [N m^{-1}]	α	β_1 [N m^{-3}]	β_2 [N m^{-5}]
FSSB	0.1	0.055	0.025	1.00×10^{6}	834	170
	0.2	0.055	0.025	1.00×10^{6}	2040	370
	0.3	0.055	0.025	1.00×10^{6}	2090	350
	0.4	0.055	0.025	1.00×10^{6}	652	110
CSSB	0.1	0.055	0.025	1.00×10^{6}	700	1000
	0.2	0.055	0.025	1.00×10^{5}	880	420
	0.3	0.055	0.025	1.00×10^{5}	889	350
	0.4	0.055	0.025	1.00×10^{5}	890	350

4. Results of the analyses

From Fig. 3 to Fig. 6, the comparison of the computed response is depicted in terms of the horizontal displacement history of the base (left plot) and the hysteresis loop (right plot) of each seismic device and for each value of the displacement limit. It can be observed that the magnitude of the horizontal displacement history is the same for all devices, accordingly the dynamic properties, i.e. the natural circular frequency of vibration, is practically the same for each device. The response in terms of angular displacement history is not an object of study since the angular displacement amplitude has turned out negligible.

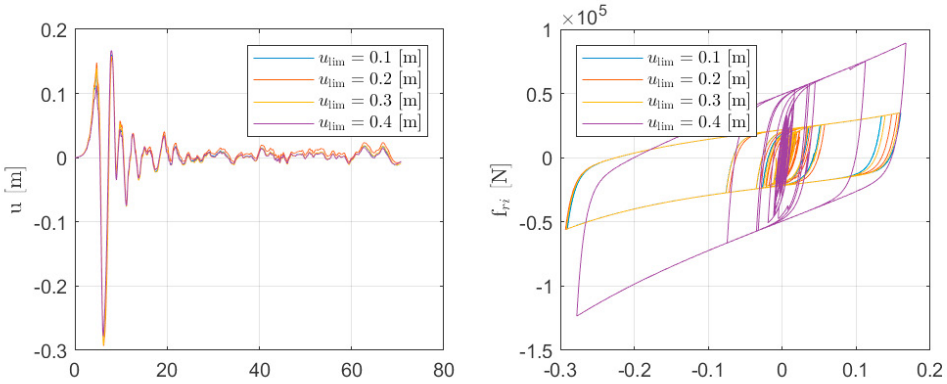

Fig. 3 - Steel Reinforced Elastomeric Bearings

In Fig. 7 the maximum displacement to limit displacement ratio is shown for each device, in fact this ratio represents a kind of safety factor. It can be observed that the safety of the object is achieved by the devices with a limit displacement ranging from 300 to 400 mm.

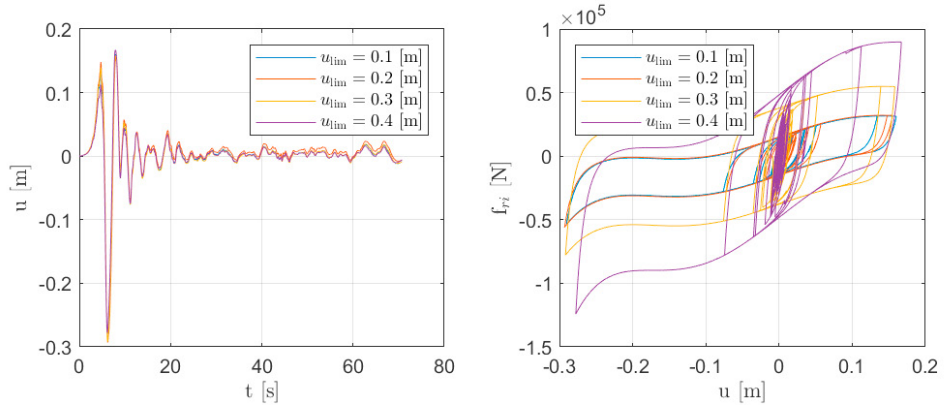

Fig. 4 - Fiber Reinforced Elastomeric Bearings

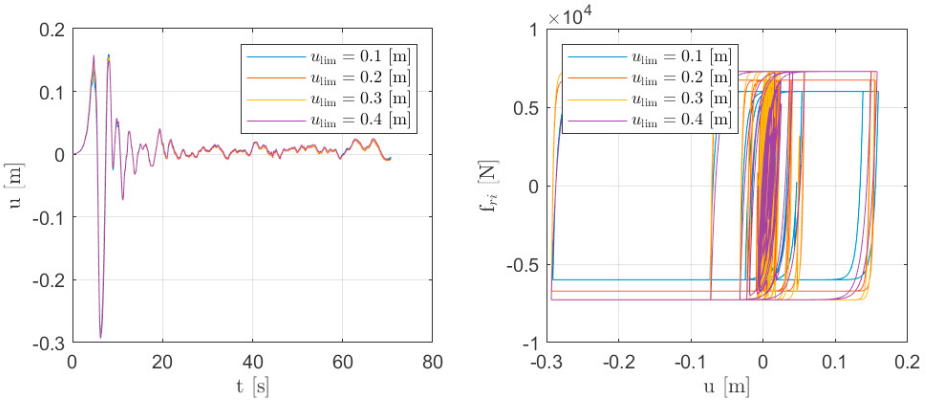

Fig. 5 - Flat Surface Sliding Bearings

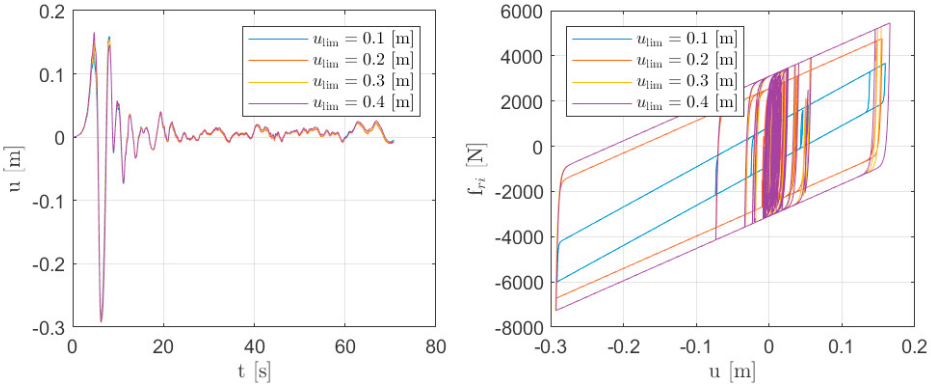

Fig. 6 - Curved Surface Sliding Bearings

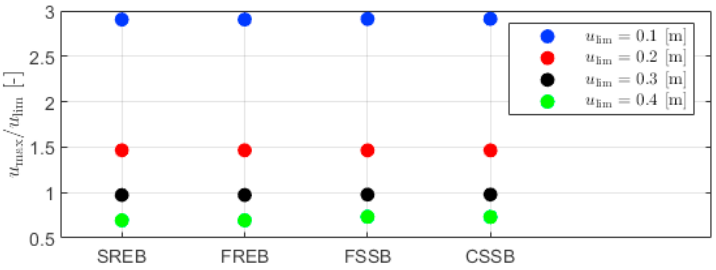

Fig. 7 - The maximum displacement to limit displacement ratio.

5. Conclusions

The nonlinear dynamic behavior of the base-isolated Riace bronze A subjected to horizontal ground acceleration has been examined. The Riace bronze A has been modeled as a symmetric rigid body that is able to rock about one of the two bottom corners, whereas the rigid base can oscillate horizontally. So, the model under this study has only two degrees of freedom. The sliding motion is prevented assuming that the coefficient of kinetic friction between the body and the rigid base is big. The collisions problem has been investigated applying the laws of conservation of linear and angular momentum, in order to evaluate the angular and horizontal velocities after the collision. The rigid base is supported by seismic isolators that have a complex hysteretic behavior, namely the elastomeric and sliding bearings that represent the main categories of seismic isolation device used to date for seismic protection of art objects. An innovative uniaxial phenomenological model has been adopted in order to predict the nonlinear behavior of such devices. The proposed hysteretic model is described by an algebraic equation that does not require iterations to evaluate the state variables, namely the device restoring forces; additionally, the proposed hysteretic model is based on a set of parameters with a clear mechanical significance. Numerical assessments have been carried out in order to

permit the comparison between the different behaviors of each isolation device analyzed in terms of horizontal displacement history and force-displacement relationship of the isolators. Moreover, the maximum displacement to limit displacement ratio has been evaluated for the purpose of estimating a safety factor.

Future research directions will include an experimental assessment of the seismic devices, which will be also performed on Wire Rope Isolators (Vaiana 2017, 2019d), whose constitutive parameters will be investigated by the procedure proposed by Sessa et al. (2020). Moreover, in order to provide a more exhaustive comparison not related to a single seismic event, the procedure will be implemented in a multi-objective random vibration analysis (see, e.g., Sessa 2010) so that seismic responses can be compared from a statistical point of view.

Acknowledgements

We are grateful to Gerardo De Canio, of Agenzia nazionale per le nuove tecnologie, l'energia e lo sviluppo economico sostenibile (ENEA), for his help regarding the geometrical properties of the Riace bronze A. Special thanks to Jean-Luc Dion and Stefania Lo Feudo, of Supméca - Institut supérieur de mécanique de Paris, for their suggestions and support with the preparation of numerical experiments.

References

Augusti, G., Sinopoli, A., 1992. Modelling the dynamics of large block structures. Meccanica 27, 195-211.

Cimellaro, G.P., Domaneschi, M., Qu, B, 2020. Overturning Risk of Furniture in Earthquake Affected Areas, Journal of Vibration and Control, 26(5-6), 362-374.

Caliò, I., Marletta, M., 2004. On the mitigation of the seismic risk of art objects: case-studies. 13th World Conference on Earthquake Engineering 2828.

Constantinou, M.C., Mokha, A., Reinhorn, A.M., 1990. Teflon bearings in base isolation. II: Modeling. Journal of Struct. Eng. 116, 455–474.

Constantinou, M.C., Whittaker, A.S., Kalpakidis, Y., Fenz, D.M., Warn, G.P., 2007. Performance of seismic isolation hardware under service and seismic loading. Report No. MCEER-07-0012, State University of New York, Buffalo, NY, USA.

De Canio, G., 2012. Marble devices for the Base isolation of the two Bronzes of Riace: a proposal for the David of Michelangelo. Proceedings XV World Conference on Earthquake Engineering-WCEE, 24-28.

Gesualdo, A., Iannuzzo, A., Guadagnuolo, M., 2016. Numerical analysis of rigid body behaviour. Applied Mechanics and Materials 847, 240-247.

Gesualdo, A., Iannuzzo, A., Monaco, M., Penta, F., 2018. Rocking of a rigid block freestanding on a flat pedestal. Journal of Zhejiang University 19, 331-345.

Gesualdo A, Iannuzzo A, Minutolo V, et al. 2018. Rocking of freestanding objects: theoretical and experimental comparisons. Journal of Theoretical and Applied Mechanics 56(4): 977–991.

Housner, G. W., 1963. The behavior of inverted pendulum structures during earthquakes. Bulletin of the Seismological Society of America 53, 403-417.

Mokha, A., Constantinou, M.C., Reinhorn, A.M., 1990. Teflon bearings in base isolation. I: Testing. Journal of Structural Engineering 116, 438–454.

Roussis, P., Pavlou, E., Pisiara, E., 2008. Base-isolation technology for earthquake protection of art objects. 14th World Conference on Earthquake Engineering, Beijing, China.

Sessa, S., Vaiana, N, Paradiso, M, Rosati, L., 2020. An inverse identification strategy for the mechanical parameters of a phenomenological hysteretic constitutive model. Mechanical Systems and Signal Processing, 139, 106622.

Sessa, S. 2010. Multiobjective non-linear random vibration analysis for performance-based earthquake engineering. Reliability and Optimization of Structural Systems - Proceedings of Reliability and Optimization of Structural Systems, 185-192.

Vaiana N, Spizzuoco M, Serino G, 2017. Wire rope isolators for seismically base-isolated lightweight structures: Experimental characterization and mathematical modeling. Engineering Structures 140(1), 498-514.

Vaiana, N., Sessa, S., Marmo, F., Rosati, L., 2018. A class of uniaxial phenomenological models for simulating hysteretic phenomena in rate-independent mechanical systems and materials. Nonlinear Dynamics 93(3), 1647-1669.

Vaiana, N., Sessa, S., Marmo, F., Rosati, L., 2019a. An accurate and computationally efficient uniaxial phenomenological model for steel and fiber reinforced elastomeric bearings. Composite Structures 211, 196-212.

Vaiana, N., Sessa, S., Paradiso, M., Rosati, L., 2019b. Accurate and efficient modeling of the hysteretic behaviour of sliding bearings. Proceedings of the 7th ECCOMAS Thematic Conference on Computational Methods in Structural Dynamics and Earthquake Engineering (COMPDYN). https://doi.org/10.7712/120119.7304.19506.

Vaiana, N., Sessa, S., Marmo, F., Rosati, L. 2019c. Nonlinear dynamic analysis of hysteretic mechanical systems by combining a novel rate-independent model and an explicit time integration method. Nonlinear Dynamics, 98(4), pp. 2879-2901.

Vaiana N, Marmo F, Sessa S, Rosati L, 2019d. Modeling of the hysteretic behavior of wire rope isolators using a novel rate-independent model. Nonlinear Dynamics of Structures, Systems and Devices. Proceedings of the First International Nonlinear Dynamics Conference (NODYCON 2019), 1, 309-317. https://doi.org/10.1007/978-3-030-34713-0_31.

Zuccaro, G., Dato, F., Cacace, F., de Gregorio, D.D., Sessa, S., 2017. Seismic collapse mechanisms analyses and masonry structures typologies: A possible correlation. Ingegneria Sismica, 34(4), 121-149.